Astronomy & Astrophysics manuscript no. eev February 2, 2008
(DOI: will be inserted by hand later)

Properties of radio pulses from lunar EeV neutrino showers

A. R. Beresnyak[1]

Puschino Radio Astronomy Observatory, Puschino,
Moscow region 142290, Russia
e-mail: beres@prao.psn.ru

Abstract. We present results of the simulation of the intensity distribution of radio pulses from the Moon due to interaction of EeV neutrinos with lunar regolith. The radiation mechanism is of coherent Ĉerenkov radiation of the negative charge excess in the shower, known as Askar'yan effect. Several realistic observational setups with ground radio telescopes are considered. Effective detector volume is calculated using maximum-knowledge Monte Carlo code, and the possibilities to set limits on the diffuse neutrino flux are discussed.

Key words. neutrinos – moon – radiation mechanisms: non-thermal

1. Introduction

Due to the lack of atmosphere on the Moon, its surface has been proposed as a target for detection of cosmic rays by mounting detectors on the Moon as early as in the original Askar'yan's papers (Askaryan, 1962, 1965). Using the whole visible lunar surface with its huge effective volume by monitoring the Moon with ground based radiotelescope has been first proposed by Dagkesamanskii & Zheleznykh, 1989. Large effective volume presumed detection of particles with extremely low fluxes, while the distance from the observer limits to the very energetic events. Using Askar'yan's effect for detection of neutrinos of cosmic rays is considered advantageous, since shower coherent radio emission grows roughly as a square of initial particle energy, and with this consideration in mind it had hoped to overcome the steep decline in flux expected from known CR spectrum. However the first rough estimates (Dagkesamanskii & Zheleznykh, 1989), has been shown to be too optimistic. This is due to the particular target geometry: neutrinos at EeV energies are expected to have rather high cross-section, and the detectable events will be only those crossing the edge of the Moon, and the fact that Ĉerenkov angle is complimentary to the full internal reflection angle.

Up to now, there has been several attempts to detect ultrashort radio pulses from the Moon (Hankins et al. 1996; Gorham et al, 2001) none of which shown any signs of such pulses. However, these observations, combined with the detailed modeling of the emission will allow to reject particular models of EeV neutrino spectrum.

Particles with energies around 10^{20}eV and higher became one of the major interest in the field of CR science since the formulation of the GZK paradox (Greisen et al, 1966; Zatsepin & Kuzmin, 1966). That is, starting with $5 \cdot 10^{19}$eV particles loose energy on the pion production interacting with CMB on scales of around 10Mpc, while the our Galaxy's or stochastic intergalactic magnetic fields is not high enough to sufficiently curve them. So we expect to see the sources of such particles which should be relatively nearby, but up to now, with around a hundred cosmic ray events detected near the GZK energy, they seem to be distributed rather uniform on the sky.

The expected sources of neutrinos with GZK energies, ranging from certain, such as GZK cosmic rays, to possible, such as AGNs and exotic – topological defects or massive relic particles, predict neutrino flux somewhat or of the order of magnitude higher than CR flux. Beyond GZK limit this difference might be even bigger, so it is no wonder that detection of extra high energy neutrinos received a considerable attention lately (Alvarez-Muñiz et al, 2000; Razzaque et al, 2002; Provorov & Zheleznykh, 1995; Buniy & Ralston, 2002; Alvarez-Muñiz & Zas, 1997, 1998; Gandhi et al, 1998).

The observation of the Moon with ground radio telescopes could either detect EeV neutrinos or put a limit on their flux. This paper studies various aspects of such observations and tries to find the most favorable setups.

Send offprint requests to: A. R. Beresnyak

2. Coherent Ĉerenkov radiation

Well known Frank-Tamm formula for particle Ĉerenkov losses in dense media, usually found in textbooks is not applicable in our case. This formula addresses the case of infinite track length, hence, inevitably, near-field region. However, the formula for finite track, in the Fraunhofer limit, has indeed been known for a long time (Tamm, 1939):

$$\frac{d^2P}{d\omega d\Omega} = \frac{ne^2\omega^2L^2}{4\pi^2c^3}\sin^2\theta\frac{\sin^2 X}{X^2}, \tag{1}$$

Here P is the *one-sided* energy spectral density radiated in a given solid angle, n is the refraction index, L is the track length, θ_c is the Ĉerenkov angle, X is the phase equaled to $n\omega L(\cos\theta_c - \cos\theta)$ [1]. The most prominent difference from the infinite track formula is in the frequency dependence with flux growing like the frequency squared, rather than the frequency in the first power.

Maxwell's equation for the infinite space filled with dielectric with permittivity of ϵ, and permeability of unity, will give the following solution for the Fourier component of the electric field

$$\boldsymbol{E}(\omega,\boldsymbol{x}) = \frac{i\omega}{c^2}\int dt'\, d^3\boldsymbol{x}' e^{i\omega t' + ik|\boldsymbol{x}-\boldsymbol{x}'|}\frac{\boldsymbol{J}_\perp}{|\boldsymbol{x}-\boldsymbol{x}'|}. \tag{2}$$

Here we defined Fourier component of $\boldsymbol{E}$ as

$$\boldsymbol{E}(\omega) = \int_{-\infty}^{\infty}\boldsymbol{E}(t)e^{i\omega t}\,dt. \tag{3}$$

In this normalization the radiated energy spectral density, similar to one presented in (1), one-sided, with negative and positive frequency parts summed will be

$$\frac{d^2P}{d\omega d\Omega} = \frac{cn}{4\pi^2}|RE(\omega)|^2. \tag{4}$$

From the first glance (2) does not contain any traces of the properties of the media. However, k here is not a variable, it is determined by the Ĉerenkov resonance condition $k = n\omega/c$. This expression can be reduced further by using Fraunhofer, or far field limit, that is, approximating $|\boldsymbol{x}-\boldsymbol{x}'|$ to the linear order and assuming a particular charge current distribution.

Since particles in a shower move mostly along one particular axis, the current density could be decently approximated by

$$\boldsymbol{J}_\perp(\boldsymbol{x},t) = Q(z)\hat{n}_\perp c\sin\theta\,\delta^3(\boldsymbol{x} - n_z ct). \tag{5}$$

And the electric field, from (2),

$$\boldsymbol{E}(\omega,\boldsymbol{x}) = \frac{i\omega}{c^2}\sin\theta\frac{e^{ikR}}{R}n_\perp\int Q(z')e^{ipz'}\,dz', \tag{6}$$

where $p = (1 - n\cos\theta)\omega/c$. The angular dependence of the electric field amplitude near Ĉerenkov angle may be seen as a Fourier transform of the longitudinal charge distribution. From here it is easy to reproduce finite track Frank-Tamm formula, (1).

This so called one-dimensional approximation works surprisingly well in describing maximum intensity at low frequencies and angular dependence (Alvarez-Muñiz et al, 2000). But, rather obviously, it fails to describe decoherence that comes from the transverse spread of the shower.

There has been several independent Monte-Carlo simulations of showers and their Ĉerenkov electric field (Zas et al, 1992; Razzaque et al, 2002; Provorov & Zheleznykh, 1995). The results are in pretty good agreement, concerning integral quantities such as the total projected (e-p) tracklength, L, which determines the field at the Ĉerenkov angle at low frequencies.

$$R|E(\omega,\theta=\theta_C)| = \frac{e\omega L\sin\theta}{c^2} \tag{7}$$

The tracklength has been shown to scale linearly with the energy of the showers, or with the electromagnetic energy in the hadronic showers. The accelerator observation of the effect (Saltzberg et al, 2001) does also comply reasonably well with this simulations.

[1] CGS units are used unless otherwise noted.

The first estimates of the decoherence from the transverse spread of the shower were done as early as in one of the pioneering Askaryan papers (Askaryan, 1965). Indeed, this issue is important for choosing the best observation frequency and for estimates of maximum coherent flux.

In the present paper we adhere to the particular parametrization for the electric field of one of these simulations, (Alvarez-Muñiz et al, 2000), assuming that tracklength, decoherence frequency and the angular width of the Ĉerenkov cone scale with radiation length.

The decoherence is described by the phenomenological form-factor fitting electric field intensity at the Ĉerenkov angle, (Alvarez-Muñiz et al, 2000),

$$F(\nu) = \frac{1}{1 + (\nu/\nu_0)^{1.44}}, \tag{8}$$

We have to note, however, that different shower MC's do not agree very well at frequencies higher than decoherence frequency, which is around 2.5GHz for regolith.

3. Showers

As we see from (6) the longitudinal profile of the shower determines the angular width and the form of the Ĉerenkov electric field peak. Showers with energies higher than 1 TeV but less than 1 PeV do not fluctuate much and have profiles close to gaussian, with longitudinal spread growing slowly with energy as $\sqrt{2/3\log(E_0/E)}$ (Rossi, 1952). Starting with energies around 10 PeV, electromagnetic showers are affected by Landau Pomeranchuk Migdal effect (Landau & Pomeranchuk, 1953; Migdal, 1956, 1957). Due to suppressed interaction at high energies the shower looks as a combination of several subshowers, with normal length, that is of several radiation lengths. The number of these subshowers are usually not enough to add up to the good averaged gaussian profile, so LPM showers fluctuate a lot. In fact, each of them has the individual form. However the Fourier transform of such a sparse showers have some general features. Namely, there are two characteristic lengths, one of the total length of the shower, and the other is 7-9 radiation lengths, the typical length of a non-LPM shower at these energies. So, the Fourier transform have an envelope inside of which there is a typical interference pattern, and the total shower length determine the width of an individual peaks.

Neutrino or antineutrino interacting with nucleon's quark by charged current ($W^{\pm}$) gives the corresponding charged lepton and changes the flavour of the quark. The charged lepton, say, the electron, then initiate electromagnetic shower of energy $(1-y)E_\nu$, and the quark initiate hadronic shower of energy yE_ν. Due to the high multiplicity of the collisions governed by strong force high initial energy in hadronic shower got divided pretty quickly, thus mitigating the LPM effect. It has been shown than some hadronic showers of energy as high as 100EeV show little or no LPM elongation, while the others are lengthening only by several tenths percent (Alvarez-Muñiz & Zas, 1998). So, the charge current interacting neutrino produces two distinctly different showers, in the case of initial electron neutrino they are develop in the same place and the Ĉerenkov electric field will be the sum of that of each of them. The neutral current (Z) interactions got neutrino scattered, and produces only hadronic shower of energy of yE_ν.

The deep inelastic scattering (DIS) cross sections for the energies in question is determined mainly by the behavior of the distribution function of the sea quarks at low values of x, such as $x \approx M_W^2/2ME_\nu y$ which is $3 \cdot 10^{-8}/y$ at $E_\nu = 10^{20}$eV. The distribution function at these x has not been measured directly, however it could be extrapolated from lower values of x by the power law with index of around -1.3 (Gandhi et al. 1998). We assumed $xq_s(x) \approx x^{-0.33}$. This parametrization gives an semianalytic expression for the $d\sigma/dy$ dependence we are interested in. For example, for muon neutrino the differential cross section is proportional to $(3 + 2(1-y)^2)y^{-0.67}$ for charged current and $(1 + (1-y)^2)y^{-0.67}$ for neutral current, mean values of y being 0.2 and 0.19 correspondingly.

In our simulation the total νN CC and NC cross sections were taken from the parametrization in (Gandhi et al. 1998), σ_{NC} being a 0.42 fraction of σ_{CC}.

4. Time dependence

Determining the time dependence of the real Ĉherenkov pulse might be a tricky matter. Even though early papers on Askaryan effect suggested using full-bandwidth ionospheric-delay compensated radio observations which will maximize signal-to-noise ratio and make use of the unique Ĉherenkov pulse shape (Dagkesamanskii & Zheleznykh, 1989), it would probably be the way only future dedicated instruments will work. All experiments up to date used a bandwidth limited, maximum flux triggered setup.

It was suggested to use the frequency domain electric field strength directly from the theory (Gorham et al, 2001), as the receiving system works with voltages, which are basically the electric field times the antenna effective height. However, certain disadvantages come with this approach. The different simulations of showers often use different fourier transform normalisation, which sometimes lead to confusion (Razzaque et al, 2002). In the real experiment voltage

is always recorded in the time domain. Also, the effective height of the antenna is not always easy to get, and the effective area may change due to orientation. In radio astronomy it is more common to calibrate receiving system with one or two strong radio sources. This calibration relates mean squared voltages with the spectral flux of the source. It is also easier to speak of decoherent weakening of the signal, such as scattering, in terms of the power, rather that the amplitude.

In a maximum flux triggered setups, used in today (GLUE) and proposed for future experiments (ANITA), the phase characteristic of the system plays a major role, while the radio astronomers are used to fluxes and usually cut several narrow bands in the primary wide band. For a gaussian characteristic of the system without phase shifts the maximum flux recorded will be the one-sided energy spectral density times $2\pi(\Delta f)_{1/2}/1.18$, in the assumption that the signal phase and amplitude do not change significantly over this band. For filters with flat top used in radio receiving systems this coefficient is lower, but more impotantly, it is hard to keep zero phase shifts over a wide bandwidth. In general, we can use the *effective response time* of the system, which is the maximum recorded flux divided by the energy spectral density of the delta-like pulse. For real systems this time might be much larger than that determined by uncertainty relation $(1/(2\pi\Delta f))$, thus making maximum flux trigger setup less effective. The calibration of the system with sufficiently short pulses is almost always neccesary for this setup.

5. Geometry and refraction

In this section, and later, in Monte Carlo, we limit ourselves with purely refracted pulses. The reason for this is that only refracted pulses, as opposed to scattered over surface roughness ones, keep their unique ultra-short time structure. The typical timescale of a pure pulse which is determined by the decoherence frequency 2.5 GHz is around 60 picoseconds, while the delays from the radiation scattered over the range of several tens of meters would be hundreds of nanoseconds. Thus, the amplitude and phase characteristics of the scattered pulses are affected down to frequencies of 100 MHz or even lower.

The solid angle of the part of the ray caught by the telescope is much smaller than the typical refracted Ĉerenkov cone, so we can use ray optics. According to the effect mentioned in the introduction there should be strong damping of the outgoing radiation, however, as it was found, the transmissivity at the regolith-vacuum interface is not much to blame. As it follows from the geometry of the most detectable events, the E vector will lay close to the plane of refraction, however the $T_\parallel$ transmission coefficient, being zero at total reflection angle, rises sharply to 1 in a few degrees.

It is the solid angle stretching near zero angles that does the most effect. Indeed, the solid angle before and after refraction will have the ratio of

$$\frac{d\Omega}{d\Omega'} = \frac{\sin\beta}{n^2 \sin\alpha},$$

where β is an angle between the plane of the surface of the Moon and the outgoing ray, and α is the same angle for incoming ray. This coefficient scales like β at small angles, as well as $T_\parallel$ does, however it is much smaller than $T_\parallel$ for the angles of a few degrees – the ones we are interested in. As an example in Figure 1 we showed the full exact damping coefficient which is the product of the above ratio to the $T_\parallel$, plotted versus $r = 1 - \cos\beta$. r may be thought of as a relative distance of the event from lunar limb, $r = 0$ correspond to the limb, $r = 1$ to the center. Both transmissivity and solid angle stretching is proportional to β at small β, however for transmissivity this law fails already at a few degrees.

It is also interesting to calculate which part of the incoming particles full 4π solid angle will give radiation coming out of the Moon, though not necessarily detectable, in the assumption that all radiation is concentrated in the cone with typical angle estimated in section 2. This "effective" solid angle is shown on figure 2. It happened, that those neutrinos that have positive entrance angles, that is those, that hit the visible hemisphere, give important income to this total angle, especially at low frequencies and low β's.

As we see from Figures 1 and 2 both the effective solid angle and the intensity damped by more than order of magnitude, which undermines previous optimistic estimates (Dagkesamanskii & Zheleznykh, 1989) and brings close attention to the detailed modeling of the transmissivity properties of the lunar-vacuum interface. In the next section we describe such a modeling.

6. Monte Carlo

We modeled a 64 meter telescope with standard circular aperture, pointed at some point between lunar center and the limb, making observations at some frequency ν with a bandwidth of 100 MHz, set up so to trigger events which have a total flux density higher than a certain threshold.

Fig. 1. The full damping at the regolith-vacuum interface, versus relative distance from the limb

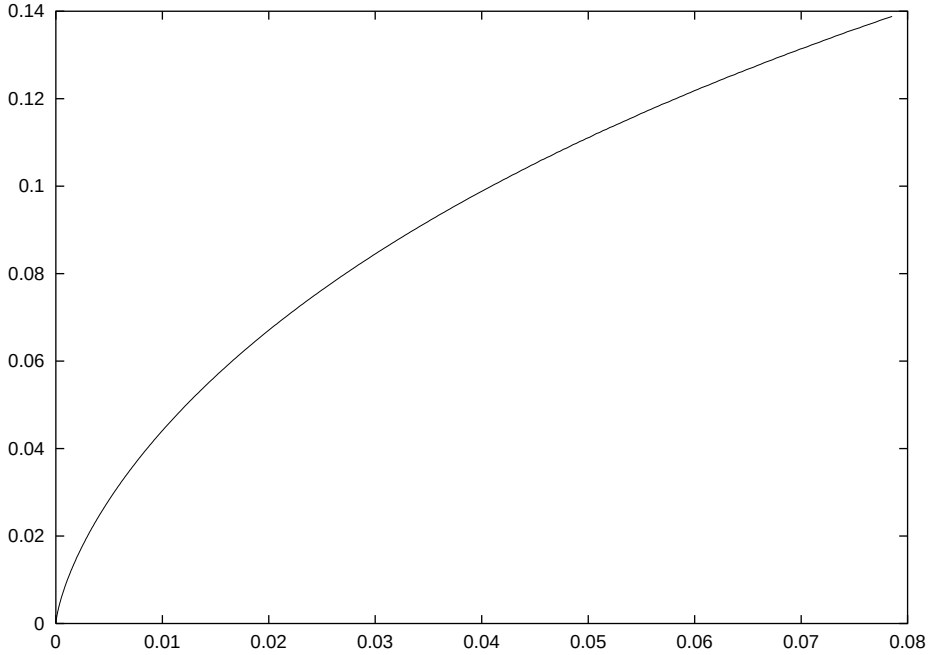

Fig. 2. The effective solid angle versus output angle, in the assumption that radiation coming from Ĉerenkov cone is always observed

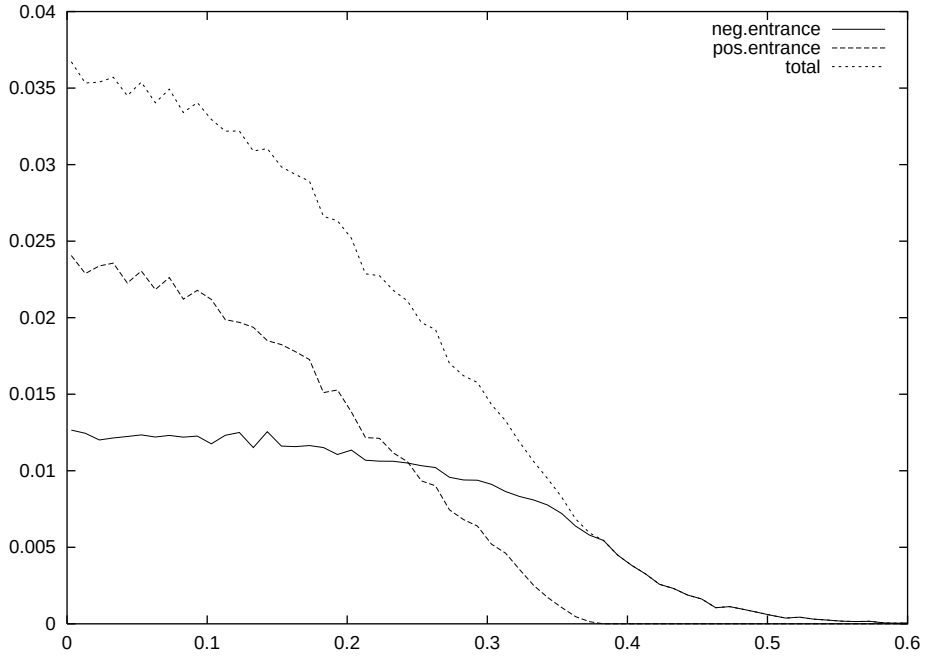

For each prospective CC or NC event we generated its lunar coordinates, depth at which interaction took place, two angles of the incoming neutrino, Bjorken y, calculated the radio flux taking into account LPM by parametrizations from (Alvarez-Muñiz & Zas, 1997, 1998) and polarization position angle. We used exact formulae for transmissivity of two different polarizations, adopted absorption length of 15 m(1 GHz/ν). We assumed that regolith or some other material with similar properties cover the Moon with a layer of at least 30 meters deep, which somewhat increased effective volume at very high energies. We adopted the lunar surface slopes model with the gaussian distribution of the slope angles with an rms of of 6^o at the length scales we are interested in. The angular dependence of the shower radio flux, and the angular dependence of the sensitivity of the telescope were both taken into account.

Fig. 3. Some events as seen on the Moon's face. Upper circle is the Moon's limb, lower shows the telescope beam. Polarization is shown with electric field vectors.

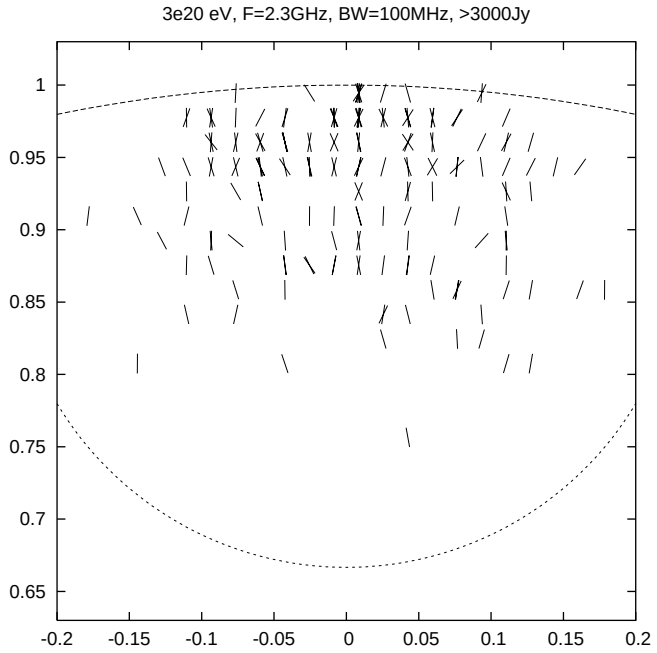

Several events with their polarizations were drawn on Figure 3. The frequency of observation was 2.3 GHz and the flux density limit 3000 Jy. The telescope was aimed $13.5'$ from the lunar center. As we see, most of the events are concentrated close to the rim, and this behavior becomes more prominent with higher energies, since the neutrino interaction length shortens. As it comes from a theory, all events are fully linearly polarized, and polarization tends to align along radius-vector to the lunar center.

Neutrinos with positive entrance angles give almost no contribution at low energies, $< 10^{20}$eV, however their relative contribution grows as cross-section grows, at 10^{23}eV contributing about the half of all trigger events.

Even though the mean value of y is around 0.2, that is most of the time most of the energy goes to either electromagnetic shower or neutrino, in this geometry electromagnetic showers happen to be relatively unimportant for radio detection. They contribute to trigger significantly only close to the edge of detection, which is around 10^{20}eV for 2.3 GHz and a bandwidth of 100 MHz. The number of triggers came purely from EM showers do not grow much with energy.

The effective detector aperture for the frequency of 2.3GHz and a limit of 3000 Jy as dependent on primary particle energy is shown on Figure 4. Also shown apertures from two GLUE publications.

We show effective apertures instead of effective volumes, traditional in neutrino experiments, for a good reason. In order to provide predictions on flux we need aperture, which is usually deduced from volume and the cross section. In our case, however, the cross section itself is under discussion, and the simulation naturally use cross sections to calculate shadowing factors. Thus, showing apertures we avoid the situation when someone use our effective volume with the cross section different from that we used.

Even though radio location of the Moon suggest the rms of the slopes to be around 6^o, the different parts of the surface has this value different. Such as the places abundant in craters have significantly higher rms slope and marines have lower ones. Hence, in the case of a large single dish and high observation frequency, when the Moon is resolved, it might be advantageous to look at the places with craters. The present ground radio techniques, however, can only measure rms of the slopes of the frontal part of the surface of the Moon, and since we almost always want to aim at the rim, these results must be taken with caution, until the lunar surface roughness is explored in more detail. On Figure 5 we show the dependence of the effective volume, as opposed to the rms of the slope in degrees, for three neutrino energies.

7. Diffuse neutrino flux limits and discussion

Having the observational time, and the effective aperture deduced in a previous section it is straightforward to estimate a diffuse neutrino flux at a given energy, having several events detected, or put an upper limit on flux if there were no detection. However, the fact of no-detection, logically, allows us to reject only one *particular* model spectrum of the

Fig. 4.

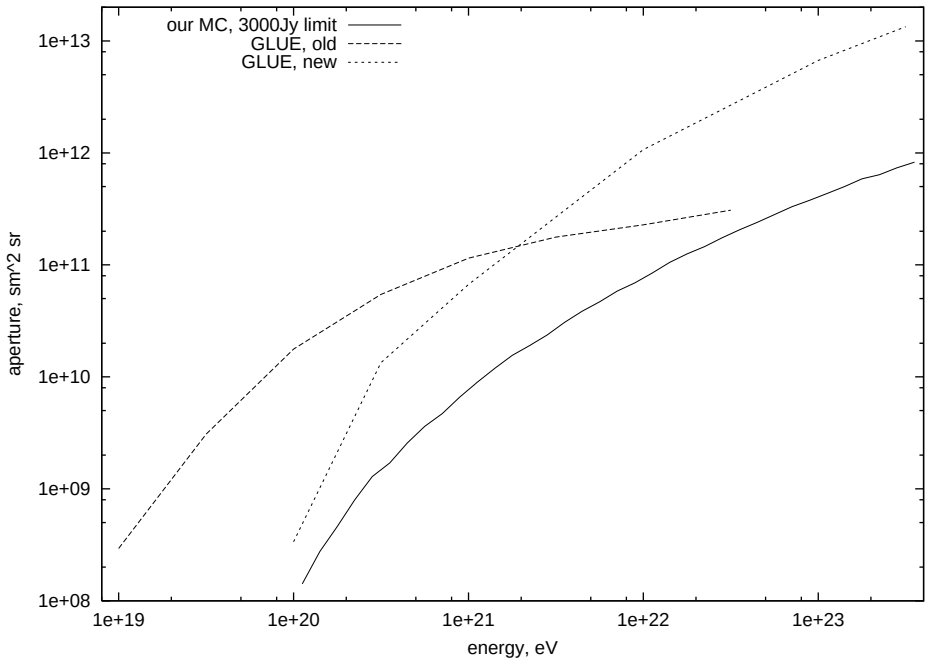

Fig. 5. Effective volume vs rms of the slopes

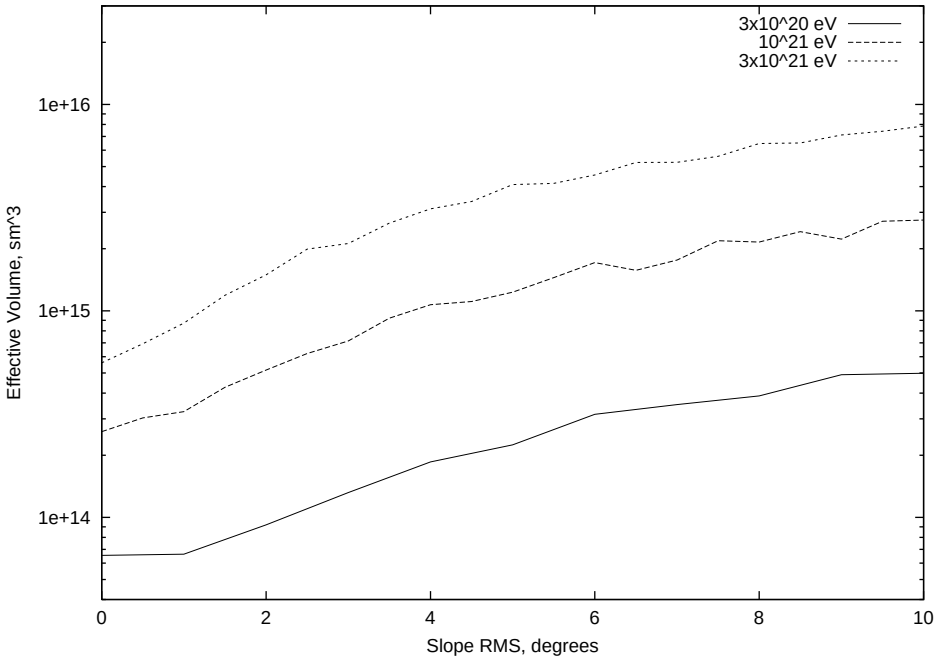

cosmic neutrinos. It allows not the upper limits on a real differential flux curve EdF/dE at any given energy. Indeed, the differential flux might have a thin but high fluke constituting only a small amount of an integrated flux, which surely will not be detected.

For the purpose of the GLUE experiment (Gorham et al, 2001) the so called model-independent limit of flux is described as the limit on the the EdF/dE curve equaled inverse of the product of aperture and the observational time, corrected by the appropriate Poisson factor for the certain confidence level. This limit is appoximately true, if the flux does not change significantly over the order of magnitude of energy. However, we propose a bit more strict limit, which is multiplied by the factor of $1/\log(\Delta E)$, thus allowing to rule out the total flux between and under two ajacent points. The closer points are, the higher will be the limit.

As we see from previous discussion, especially from figure 4, the lunar neutrino experiments, such as GLUE, or Pushchino experiment are rigged with uncertanty in the interpretation. Even the estimates of the aperture given by the same group changes significantly. In the case of purely refracted pulses considered in this article, the biggest uncertanty is in the fact, that we do not know exactly neither the distribution of the slopes, nor the number of the pulses that will be refracted purely, as opposed by scattered by small irregularities of the surface.

Acknowledgements. I am grateful to R. D. Dagkesamanskii and I. M. Zheleznykh for fruitful discussion and suggestions. This work was partially supported by Russian Foundation of Base Research grant N 02-02-17229.

References

Alvarez-Muñiz J.; Vázquez R. A.; Zas E., 2000, Phys. Rev. **D**,**62**,063001
Alvarez-Muñiz J., Zas E., 1997, Phys.Lett. B411, 218-224
Alvarez-Muñiz J., Zas E., 1998, Phys.Lett. B434, 396-406
Askaryan G.A., 1962, JETP 14, 441
Askaryan G.A., 1965, JETP 21, 658
Buniy R.V., Ralston J.P., 2002, Phys.Rev. **D 65**, 016003
Butkevich A.V., et al, 1988, Z. Phys. C, **39**, 241-250
Dagkesamanskii R.D., Zheleznykh I.M., 1989, JETP Lett, 50, 233
Gandhi R., et al, 1998, Phys.Rev. D **58**, 093009
Gorham P.W., et al, 2001, Proc. RADHEP-2000, p.177.
Greisen K., 1966, Phys. Rev. Lett. **16**, 748
Hankins T.H., Ekers R.D., O'Sullivan J.D., 1996, MNRAS, 283, 1027.
Landau L., Pomeranchuk I., 1953, *Dokl. Akad. Nauk SSSR* **92**, 535; **92**, 735
Migdal A. B., 1956, Phys. Rev. **103**, 1811
Migdal A. B., 1957, Sov. Phys. JETP **5**, 527
Provorov A. L. and Zheleznykh I. M., 1995, Astropart. Phys. 4, 55
Razzaque S., et al, 2002, Phys. Rev. **D**, **65**, 103002
Rossi B., 1992, High Energy Particles (Prentice Hall, New York)
Saltzberg D., Gorham P.W., et al., 2001, Phys. Rev. Lett., **86**, 13, 2802.
Tamm I.E., 1939, J. Phys. (Moscow) 1, 439
Zas E., Halzen F., and Stanev T., 1992, Phys. Rev. **D**, **45**, 362
Zatsepin G.T., Kuzmin V.A., 1966, Pisma Zh. Eksp. Teor. Fiz. **4**, 114